

## Layered Aluminosilicate/Chromophore Nanocomposites and Their Electrostatic Layer-by-Layer Assembly

Dong Wook Kim,<sup>†</sup> Alexandre Blumstein,<sup>\*,‡</sup>  
Jayant Kumar,<sup>†</sup> and Sukant K. Tripathy<sup>†,‡,§</sup>

Center for Advanced Materials and Department of  
Chemistry, University of Massachusetts Lowell,  
Lowell, Massachusetts 01854

Received June 27, 2000

Revised Manuscript Received October 17, 2000

The formation of intercalation complexes using layered lattices is a well-known strategy for the synthesis of organic/inorganic nanocomposites. Molecules with appropriate structural features upon intercalation can preserve/exhibit a number of specific properties such as photocatalysis,<sup>1–3</sup> photoluminescence,<sup>4–13</sup> photochromism,<sup>14–16</sup> optical nonlinearity,<sup>17</sup> among others.<sup>18</sup> One of the more important features of layered lattices such as montmorillonite or hectorite is their expandable nature. Intercalation of guest molecules into such host lattices can lead to their ordered molecular arrangement. In addition, organic molecules confined to interlamellar spaces of host lattices are often characterized by improved thermal and oxidative stability due to reduced thermal motion and a quasi-absence of oxygen.<sup>19–22</sup>

Nanocomposites of organic laser dye complexes of aluminosilicates are promising because they may dis-

play a high degree of molecular orientational order of the dye molecules and a potential for enhanced electro-optical properties.<sup>18,23,24</sup> An enhancement of quantum efficiency of fluorescence can be achieved by a careful tuning of host–guest interactions. Recent investigations involving a thiophene dye guest and perovskite-metal halide host showed that such systems are promising for efficient electroluminescent devices.<sup>25</sup>

Practical limitation of layered aluminosilicates in applications to devices is their powdery nature. The conventional route to film formation is casting of an aqueous dispersion of the aluminosilicate, followed by careful drying in air. However, the thickness of the film and orientation of particles within the film are difficult to control using this approach. Given the strong negative surface charge of layered aluminosilicates, the layer-by-layer assembly using a positively charged polyelectrolyte is very appealing. Layer-by-layer self-assembly between oppositely charged polyelectrolytes is a simple route to precisely controlled functional nanometer-scale composites and has been used for the preparation of photonic materials.<sup>26–28</sup> This technique has also been employed to incorporate chromophoric subunits into the multilayer films.<sup>29–33</sup> Several reports show that this technique is adaptable for the preparation of thin nanocomposite films from a cationic polyelectrolyte and a negatively charged aluminosilicate.<sup>34–43</sup> Films obtained in this manner may be highly oriented and their surface may be extended to macroscopic dimensions.

In this work, nanocomposites containing a layered aluminosilicate with an expandable lattice such as hectorite and a coumarin dye were prepared. By alternate adsorption of positively charged polyelectrolyte and a negatively charged hectorite/coumarin complex, a

\* To whom correspondence should be addressed.

<sup>†</sup> Center for Advanced Materials.

<sup>‡</sup> Department of Chemistry.

<sup>§</sup> Tragically deceased.

- (1) Yoneyama, H.; Haga, S.; Yamanaka, S. *J. Phys. Chem.* **1989**, *93*, 4833.
- (2) Ooka, C.; Akita, S.; Ohashi, Y.; Horiuchi, T.; Suzuki, K.; Komai, S.-I.; Yoshida, H.; Hattori, T. *J. Mater. Chem.* **1999**, *9*, 2943.
- (3) Yoshida, H.; Kawase, T.; Miyashita, Y.; Murata, C.; Ooka, C.; Hattori, T. *Chem. Lett.* **1999**, *8*, 715.
- (4) Endo, T.; Nakada, N.; Sato, T.; Shimada, M. *J. Phys. Chem. Solids* **1989**, *50*, 133.
- (5) Villemure, G.; Detellier, C.; Szabo, A. G. *Langmuir* **1991**, *7*, 1215.
- (6) Ogawa, M.; Aono, T.; Kuroda, K.; Kato, C. *Langmuir* **1993**, *9*, 1529.
- (7) Tapia Estevez, M. J.; Lopez Arbeloa, F.; Lopez Arbeloa, T.; Lopez Arbeloa, I. *Langmuir* **1993**, *9*, 3629.
- (8) Lopez Arbeloa, F.; Tapia Estevez, M. J.; Lopez Arbeloa, T.; Lopez Arbeloa, I. *Langmuir* **1995**, *11*, 3211.
- (9) Włodarczyk, P.; Komarneni, S.; Roy, R.; White, W. B. *J. Mater. Chem.* **1996**, *6*, 1967.
- (10) Lopez Arbeloa, F.; Lopez Arbeloa, T.; Lopez Arbeloa, I. *Trends Chem. Phys.* **1996**, *4*, 191.
- (11) Lopez Arbeloa, F.; Tapia Estevez, M. J.; Lopez Arbeloa, T.; Lopez Arbeloa, I. *Clay Miner.* **1997**, *32*, 97.
- (12) Takahashi, Y.; Kimura, T.; Kato, Y.; Minai, Y. *Environ. Sci. Technol.* **1999**, *33*, 4016.
- (13) Momiji, I.; Yoza, C.; Matsui, K. *J. Phys. Chem. B* **2000**, *104*, 1552.
- (14) Takagi, K.; Kurematsu, T.; Sawaki, Y. *J. Chem. Soc., Perkin Trans. 2* **1991**, *10*, 1517.
- (15) Tomioka, H.; Itoh, T. *J. Chem. Soc., Chem. Commun.* **1991**, *7*, 532.
- (16) Ogawa, M. *Chem. Mater.* **1996**, *8*, 1347.
- (17) Janeba, D.; Capkova, P.; Weiss, Z. *J. Mol. Model.* **1998**, *4*, 176.
- (18) Ogawa, M.; Kuroda, K. *Chem. Rev.* **1995**, *95*, 399.
- (19) Blumstein, A. *J. Polym. Sci.* **1965**, *A3*, 2665.
- (20) Mehrotra, V.; Giannelis, E. P.; Ziolo, R. F.; Rogalskyj, P. *Chem. Mater.* **1992**, *4*, 20.
- (21) Gilman, J. W.; Morgan, A. *Recent Adv. Flame Retard. Polym. Mater.* **1999**, *10*, 56.
- (22) Dultz, S.; Bors, J. *Appl. Clay Sci.* **2000**, *16*, 15.

- (23) Endo, T.; Sato, T.; Shimada, M. *J. Phys. Chem. Solids* **1986**, *47*, 799.
- (24) Włodarczyk, P.; Komarneni, S.; Roy, R.; White, W. B. *J. Mater. Chem.* **1996**, *6*, 1967.
- (25) Chondroudis, K.; Mitzi, D. B. *Chem. Mater.* **1999**, *11*, 3028.
- (26) Decher, G. *Science* **1997**, *277*, 1232.
- (27) Wang, X. G.; Balasubramanian, S.; Li, L.; Jiang, X. L.; Sandman, D. J.; Rubner, M. F.; Kumar, J.; Tripathy, S. K. *Macromol. Rapid Commun.* **1997**, *18*, 451.
- (28) He, J.-A.; Samuelson, L.; Li, L.; Kumar, J.; Tripathy, S. K. *Langmuir* **1998**, *14*, 1674.
- (29) Cooper, T. M.; Campbell, A. L.; Crane, R. L. *Langmuir* **1995**, *11*, 2713.
- (30) Laschewsky, A.; Mayer, B.; Wischerhoff, E.; Arys, X.; Bertrand, P.; Delcor, A.; Jonas, A. *Thin Solid Films* **1996**, *284–285*, 334.
- (31) Ariga, K.; Lvov, Y.; Kunitake, T. *J. Am. Chem. Soc.* **1997**, *119*, 2224.
- (32) He, J.-A.; Samuelson, L.; Li, L.; Kumar, J.; Tripathy, S. K. *J. Phys. Chem. B* **1998**, *102*, 7067.
- (33) Kim, J.; Wang, H.-C.; Kumar, J.; Tripathy, S. K.; Chittibabu, K. G.; Cazeca, M. J.; Kim, W. *Chem. Mater.* **1999**, *11*, 2250.
- (34) Kleinfeld, E. R.; Ferguson, G. S. *Science* **1994**, *265*, 370.
- (35) Ferguson, G. S.; Kleinfeld, E. R. *Adv. Mater.* **1995**, *7*, 415.
- (36) Kleinfeld, E. R.; Ferguson, G. S. *Chem. Mater.* **1995**, *7*, 2327.
- (37) Kleinfeld, E. R.; Ferguson, G. S. *Chem. Mater.* **1996**, *8*, 1575.
- (38) Fendler, J. H. *Chem. Mater.* **1996**, *8*, 1616.
- (39) Lvov, Y.; Ariga, K.; Ichinose, I.; Kunitake, T. *Langmuir* **1996**, *12*, 3038.
- (40) Laschewsky, A.; Wischerhoff, E.; Kauranen, M.; Persoons, A. *Macromolecules* **1997**, *30*, 8304.
- (41) Kotov, N. A.; Haraszti, T.; Turi, L.; Zavala, G.; Geer, R. E.; Dekany, I.; Fendler, J. H. *J. Am. Chem. Soc.* **1997**, *119*, 6821.
- (42) Kotov, N. A.; Magonov, S.; Tropsha, E. *Chem. Mater.* **1998**, *10*, 886.
- (43) Van Duffel, B.; Schoonheydt, R. A.; Grim, C. P. M.; De Schryver, F. C. *Langmuir* **1999**, *15*, 7520.

multilayered film was fabricated on a glass substrate. Hectorite with a cation exchange capacity (CEC) of 0.44 mequiv/g (Source Clay Minerals Repository, University of Missouri) was selected as a host lattice because of its low content of  $\text{Fe}^{3+}$  impurities, which are known to quench fluorescence and are abundant in other expandable aluminosilicates. Coumarin 1 (7-diethylamino-4-methyl coumarin) (Aldrich, dye laser grade) was chosen as a guest dye because of its flat molecular shape, large dipole moment, and a high quantum yield of fluorescence. The coumarin dye was protonated by acid treatment and then intercalated into the aluminosilicate galleries by an ion exchange reaction.<sup>44</sup>

Hectorite/coumarin composites were suspended in deionized water at a concentration of 0.05 wt %, shaken overnight, and sonicated for 4 h to generate fine particles. An aqueous solution of poly(diallyldimethylammonium chloride) (PDAC) was used for growth of polycation layers. Composite/polyelectrolyte multilayers were deposited on glass substrates hydrophilized with 1% Chem-solv solution (aqueous alkaline alcohol) treatment.<sup>45</sup> The overall process of layer-by-layer deposition consisted of a cyclic repetition of the following steps: (1) a small amount of an aqueous PDAC solution (0.01 M) was deposited dropwise to cover the whole surface of the glass substrate (~1 cm by 2.5 cm); (2) after 2 min, the substrate was rinsed with deionized water and dried by blowing of dry nitrogen; (3) a few drops of an aqueous dispersion of hectorite/coumarin composite were then deposited on the PDAC layer; (4) after 2 min, the surface was rinsed again with deionized water and dried in a stream of nitrogen. The buildup of a multilayered film was monitored by UV/vis absorption spectroscopy.

Figure 1 shows the X-ray powder diffraction patterns for pristine hectorite as well as for composites of hectorite with varying dye content, intercalated with coumarin.<sup>46</sup> In Table 1, the intercalated dye content and interlayer spacing ( $\Delta d$ ) for various hectorite/coumarin composites are summarized. The interlamellar thickness of the composite is estimated from  $\Delta d = d$ -spacing - 0.96 (nm). For sample 1, the  $\Delta d$  is 0.38 nm at a coumarin content of 11% of the CEC or 1.1 wt % of the complex. As one can see,  $\Delta d$  changes little with the increase of the coumarin content below 100% of the

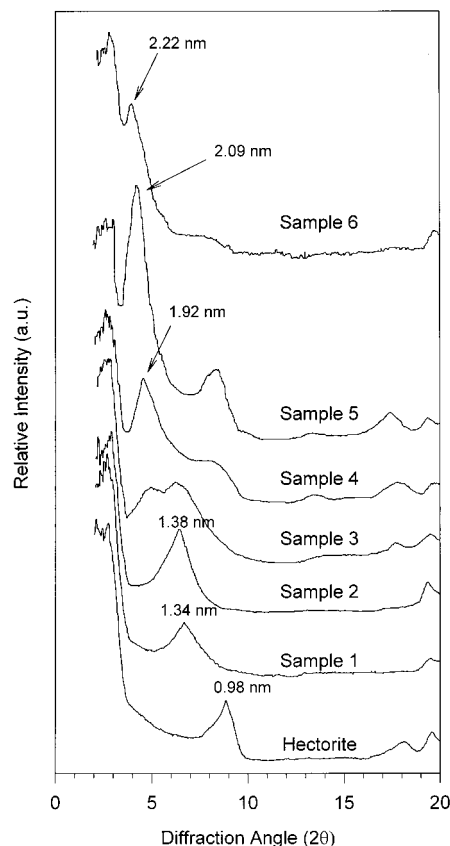


**Figure 1.** X-ray powder diffraction patterns of hectorite and hectorite/coumarin composites at different intercalated dye contents.

**Table 1. Intercalated Dye Content and the Corresponding Interlayer Spacing ( $\Delta d$ )**

sample	content of dye		$\Delta d^a$ (nm)
	wt % of complex	% of CEC	
1	1.1	11	0.38
2	6.9	73	0.42
3	10.4	114	0.43, 0.80 <sup>b</sup>
4	14.2	163	0.96
5	18.3	220	1.13
6	20.4	252	1.26

<sup>a</sup>  $\Delta d = d$ -spacing - 0.96 (nm). The error range of the  $\Delta d$  is  $\pm 0.05$  nm. <sup>b</sup> The XRD pattern for sample 3 shows two peaks, as can be seen in Figure 1.

(44) A typical procedure for preparation of the nanocomposite is as follows: 5 mL of 0.2 N hydrochloric acid was added to a solution of coumarin 1 (0.2313 g) in a mixture of methanol and deionized water (1/2 v/v). The resulting solution was stirred at 60 °C for 2 h to protonate the dye. The suspension of hectorite (2.278 g) in water was then added to the dye solution, followed by stirring for 24 h. The hectorite/coumarin composite was separated from the solution by centrifugation and washed several times with deionized water to exclude the remaining free dye trapped between the aggregates of clay particles. The resulting slurry was freeze-dried to yield a yellowish composite (sample 2, see Table 1) intercalated with the coumarin dye. The content of coumarin molecules intercalated in hectorite was determined by TGA.

(45) The glass substrate was treated as follows: the glass substrate was washed with 1% Chem-solv solution in deionized water under sonication to generate negative charges on the surface. After this treatment the substrate was rinsed several times with deionized water. Deionized water from a Milli-Q system with resistivity > 18.2 M $\Omega$ /cm and total organic content < 10 ppb was used. (See refs 31 and 33.)

(46) Since water strongly interacts with the negatively charged lamellar platelets of the hectorite, composites were manipulated and stored in an anhydrous environment. The clay samples were dried at 100 °C for at least 2 h before X-ray data were taken and the sample holder was hermetically sealed with a 6- $\mu$ m-thick polypropylene film. The  $d$ -spacing of the pure dried hectorite was thus found to be 0.98 nm, close to the theoretical value of 0.96 nm, confirming the effectiveness of the seal.

CEC. The molecular size and the cross-sectional area of coumarin dye are estimated to be  $0.32 \times 1.04 \times 0.75$  nm and  $0.78 \text{ nm}^2$ , respectively.<sup>4</sup> As long as the coumarin content does not exceed 100% of the CEC, the interlamellar thicknesses of samples 1 and 2 are consistent with the thickness of the coumarin molecule oriented "flat" or parallel to the basal planes of aluminosilicate as illustrated in Figure 2a.

When the dye content exceeds 100% of CEC, an increase in the  $\Delta d$  can be observed. The XRD pattern of sample 3 is split into two peaks ( $\Delta d = 0.43, 0.80$  nm), indicating that dye molecules within the complex may have two different orientations. One peak appears equivalent to the peak of sample 2 ("flat" orientation). The other appears similar to the peak of sample 4 and can be interpreted by two possible geometrical arrangements. One possible configuration is a bilayer of molecules oriented flat. However, the experimental value of  $\Delta d$  of 0.80 nm is not in favor of such a model. The

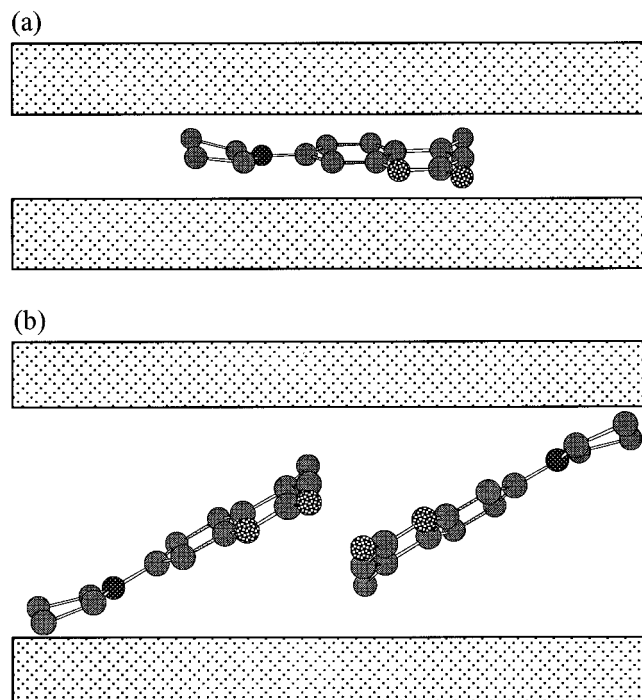
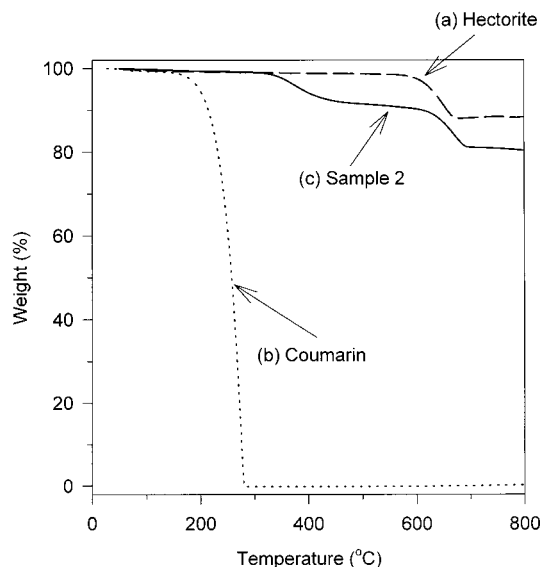


**Figure 2.** Schematic illustration of the geometrical arrangement of coumarin molecules intercalated into the hectorite with a dye content (a) below 100% of the CEC and (b) over 100% of the CEC.

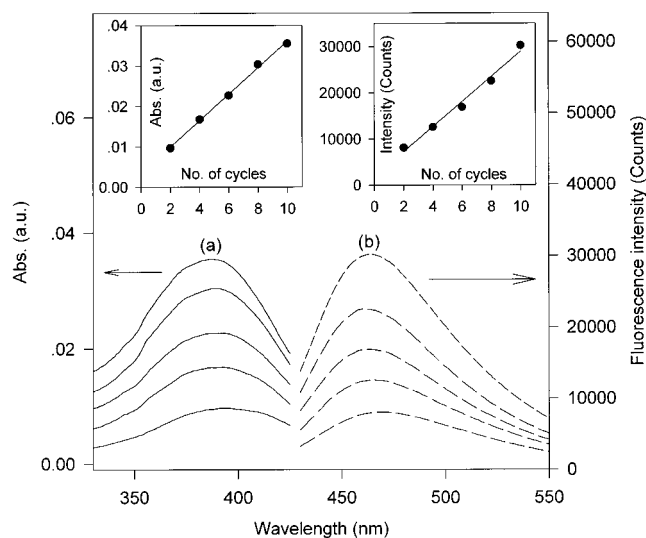
other configuration involves a tilted bilayer as shown in Figure 2b. This model appears to be in agreement with the experimental values of  $\Delta d$  and percentage of coumarin content. Hence, the biphasic structure of sample 3 seems to point toward a partial reorientation of the intercalated dye molecules to satisfy the increase of the packing of guest molecules. For the higher dye content samples, such as 4, 5, and 6, the continuing but slower expansion of the lattice could be interpreted as a progressive formation of a molecular bilayer with a tilt angle increasing with the dye content. If this view is correct, one may be able to control the orientation of the coumarin molecules by adjusting the dye content.

Figure 3 shows the results of thermal analysis for coumarin, dehydrated hectorite, and hectorite/coumarin composite. Weight loss in the composite upon heating was observed at about 350 and 600 °C. The latter corresponds to the decomposition of structural hydroxyl groups in the aluminosilicate, while the former is due to coumarin. For the intercalated coumarin the onset of weight loss was not observed until 340 °C, while for the pristine dye it began at 150 °C. Additional evidence for thermal stability of the intercalated dye molecules was provided by the isothermal degradation test (not shown). There was no detectable weight loss for the composite at 220 °C in nitrogen for over 20 h. Even at 250 °C, only ~1.5% weight loss was observed over 20 h. This remarkable enhancement of thermal stability of intercalated coumarin molecules is attributed to their restricted mobility and their spatial confinement in the silicate galleries.

A multilayered film was prepared by alternate adsorption of positively charged PDAC and negatively charged hectorite/coumarin composite on glass substrates by layer-by-layer adsorption. Figure 4a shows the absorbance change of the film with the number of



**Figure 3.** TGA of (a) hectorite, (b) coumarin dye, and (c) sample 2. The samples were heated to 800 °C at 10 °C/min in a nitrogen atmosphere.



**Figure 4.** Sequential change in the (a) UV/vis absorption spectrum and (b) fluorescence spectrum of a multilayered film on a glass substrate with the number of adsorption cycles from PDAC (0.01 M solution) and sample 2 (0.05 wt % aqueous dispersion). The insets show a linear increase of both absorbance and fluorescence intensity with the number of sequential cycles, respectively.

build-up cycles from PDAC (0.01 M aqueous solution) and sample 2 (0.05 wt % aqueous dispersion). Assuming that the absorbance intensity is proportional to the concentration of dye molecules, the buildup of a multilayered film can be estimated from UV/vis absorption spectroscopy. As shown, the multilayer adsorption of the PDAC/composite assemblies is linear and reproducible with sequential deposition. The absorbance at 390 nm is observed to increase linearly with the number of cycles, as shown in the inset (top left one) of Figure 4. These results confirm that the PDAC/composite film has built up linearly with the number of adsorption cycles. The fluorescence spectra of the PDAC/composite multilayered films with different number of deposition cycles excited at 386 nm were also measured (Figure 4b). The nanocomposite film shows a blue emission

centered at 465 nm and the intensity of fluorescence increases linearly with the number of sequential deposition cycles.

The preparative method described here offers a simple but powerful strategy for preparing a nanocomposite film with high molecular order and thermal stability for photonic applications. With adjustment of the intercalated dye content, the orientation of the dye molecules was changed from "flat" to tilted with respect to the silicate layer. The intercalated dye molecules are characterized by exceptional thermal stability. A multilayered composite film built by layer-by-layer adsorption using a cationic polyelectrolyte has displayed a linear

increase in the absorption and in the fluorescence intensity with the number of deposition cycles. This method may be adaptable to other photofunctional chromophores and fluorophores.

**Acknowledgment.** We thank Mr. M. Downey for XRD measurement and helpful discussions. D.W. Kim would like to acknowledge the support from the Korea Science and Engineering Foundation (KOSEF). This work was supported by the Petroleum Research Fund (ACS-PRF 33819-AC5,7).

CM000534Z